α-ketoglutarate coordinates carbon and nitrogen utilization via Enzyme I inhibition

Christopher D Doucette, David J Schwab, Ned S Wingreen, and Joshua D Rabinowitz

Supplementary Results

Supplementary Methods

Supplementary References

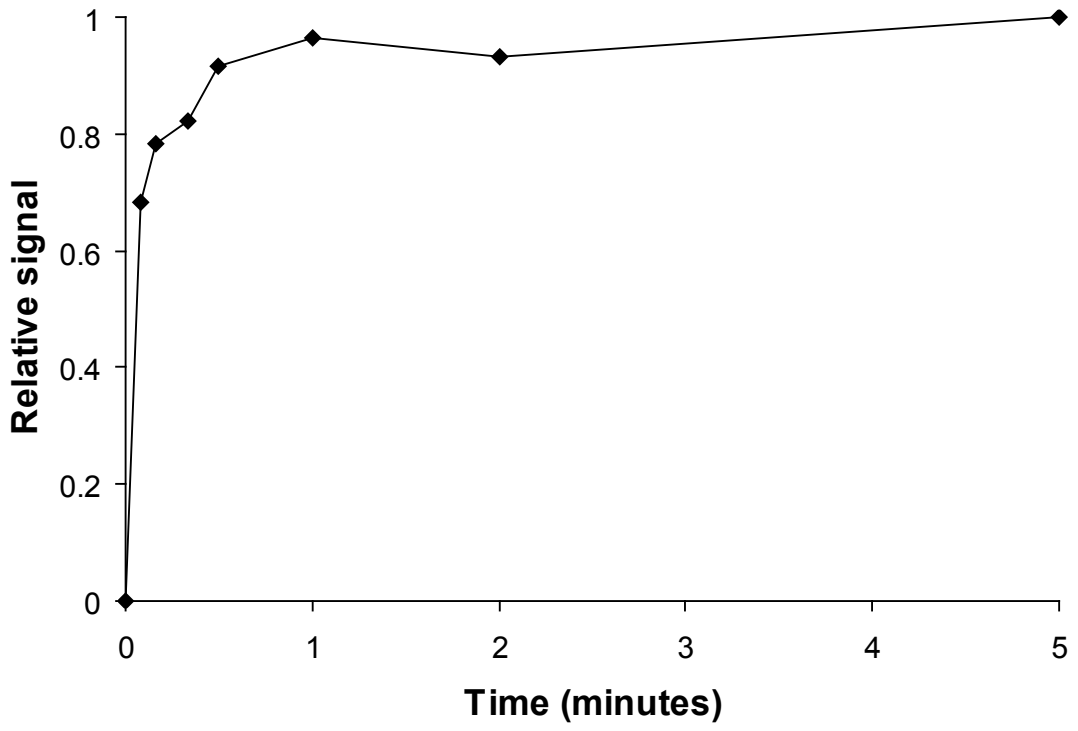

Supplementary Figure 1. Intracellular conversion of dimethyl-ketoglutarate to α-ketoglutarate.

Filter cultures were grown to mid-logarithmic phase on agarose media containing universally ^{13}C-labeled glucose and 10 mM NH_4Cl, and then transferred to similar media also containing ^{12}C dimethyl-ketoglutarate. Plotted here is the relative ^{12}C α-ketoglutarate concentration in metabolite extracts from these cells, determined by LC-MS on an Exactive orbitrap mass spectrometer (ThermoFisher Scientific).

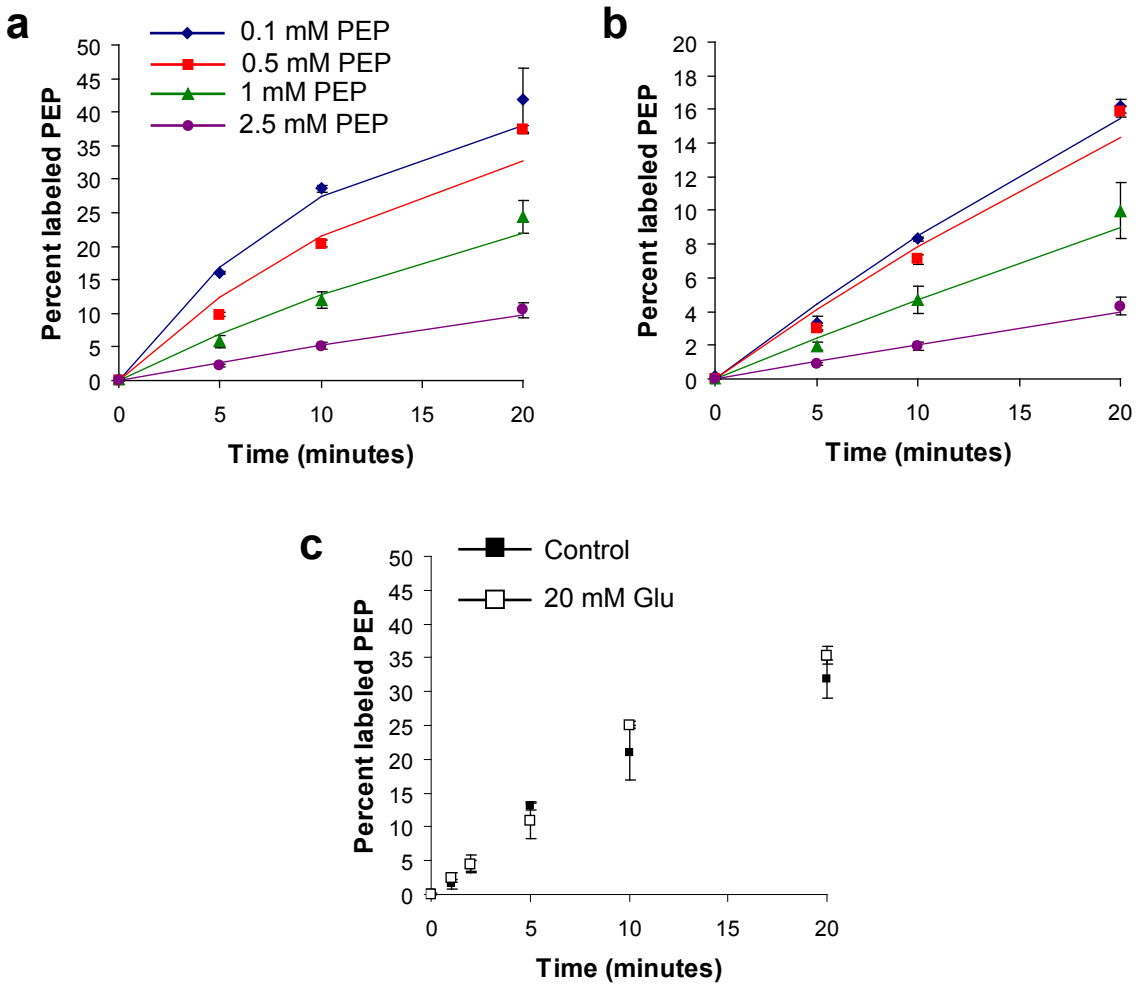

Supplementary Figure 2. Time courses of Enzyme I PEP labeling experiments. (a,b) The time-dependent fraction of ^{13}C-labeled PEP is shown here for each reaction whose rate is plotted in Figure 3a of the main text. Reactions in (a) contain no α-ketoglutarate, while those in (b) contain 2 mM α-ketoglutarate (note the change in vertical scale). Plotted points are the mean ± standard error of 3 experiments; solid lines are the best fit by weighted non-linear least squares regression, as described in Methods in the main text. (c) Time-dependent PEP labeling in reactions with and without 20 mM glutamate. Plotted points are the mean ± standard error of 3 experiments.

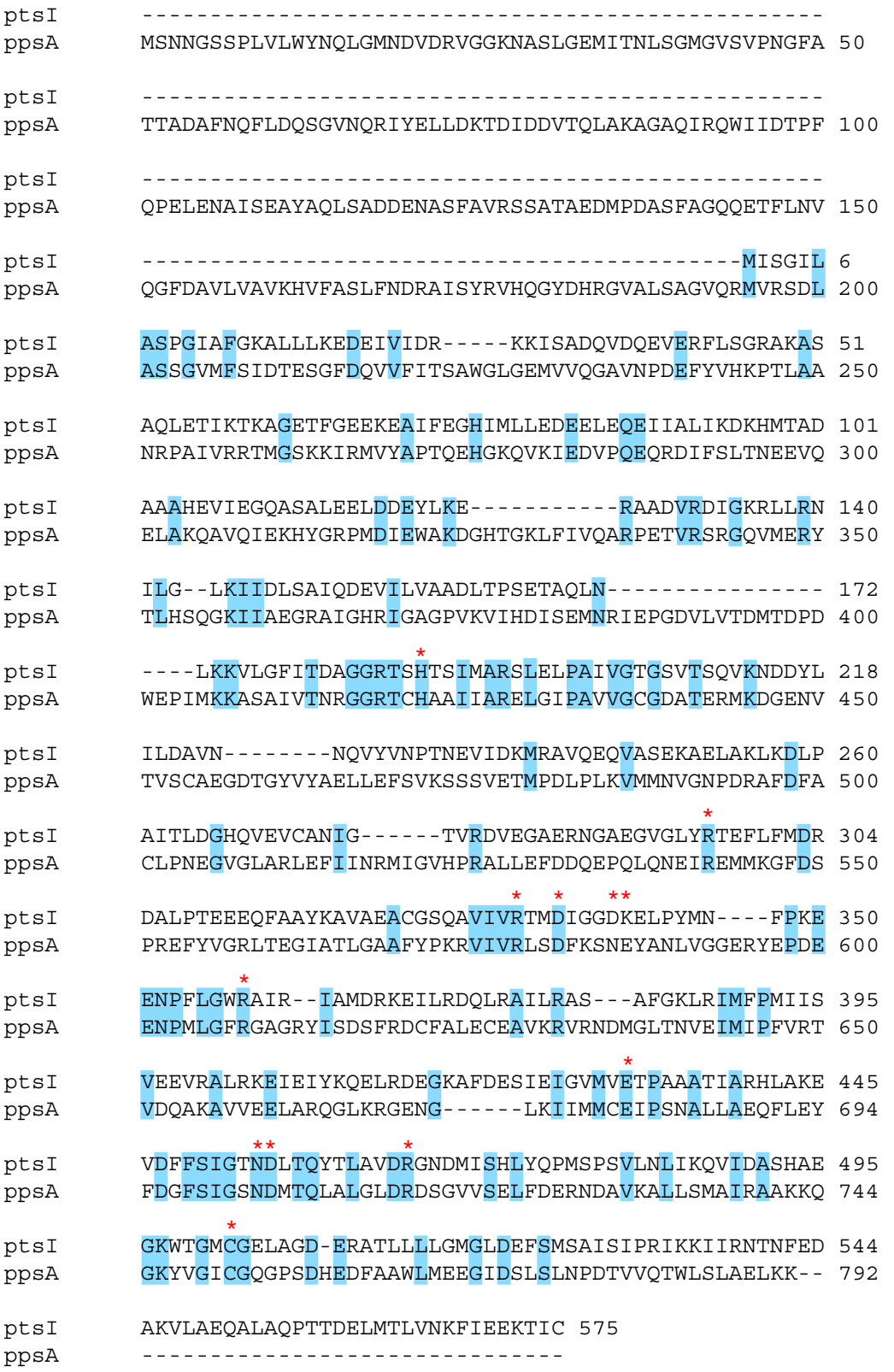

Supplementary Figure 3. Sequence alignment of Enzyme I (PtsI) and phosphoenolpyruvate synthetase (PpsA). The amino acid sequences of PtsI and PpsA were aligned in ClustalW (http://www.ebi.ac.uk/Tools/msa/clustalw2) . Exactly conserved residues are highlighted in blue. Residues in the active site of PtsI as reported in Teplyakov *et al.* 2006 are denoted by red asterisks[1].

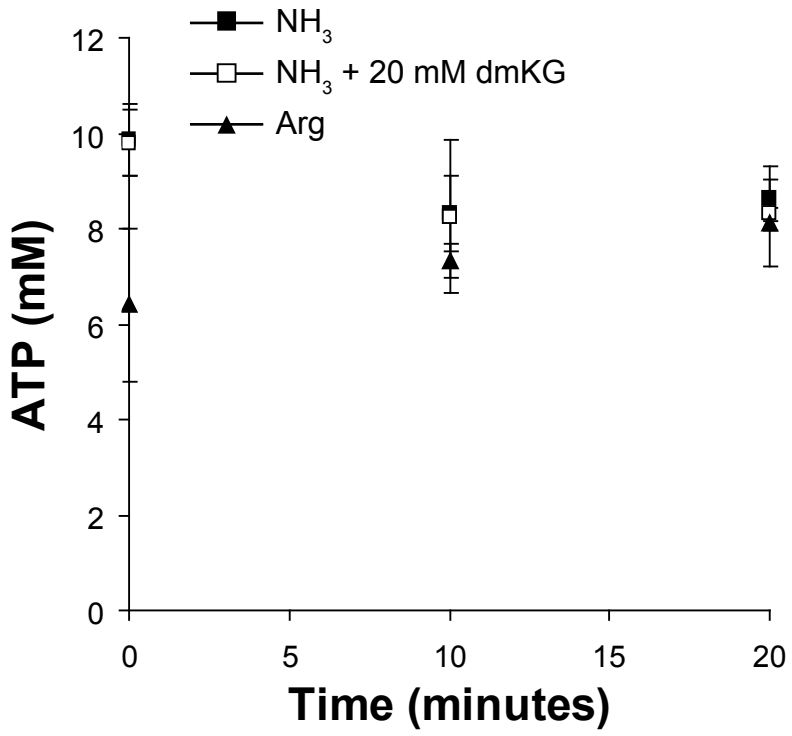

Supplementary Figure 4. ATP is not depleted during carbon downshifts. ATP concentration was monitored by LC-MS/MS during the experiments described in Figure 3c: at $t = 0$, cells were switched from media containing 4 g/L glucose as the carbon source to media containing 4 g/L glycerol. The nitrogen source was 10 mM ammonia (NH_3) or 2.5 mM arginine (Arg) as specified, and where indicated 20 mM dimethyl-ketoglutarate (dmKG) was present in the glycerol-containing media. Plotted values are the mean and standard error of 3 biological replicates.

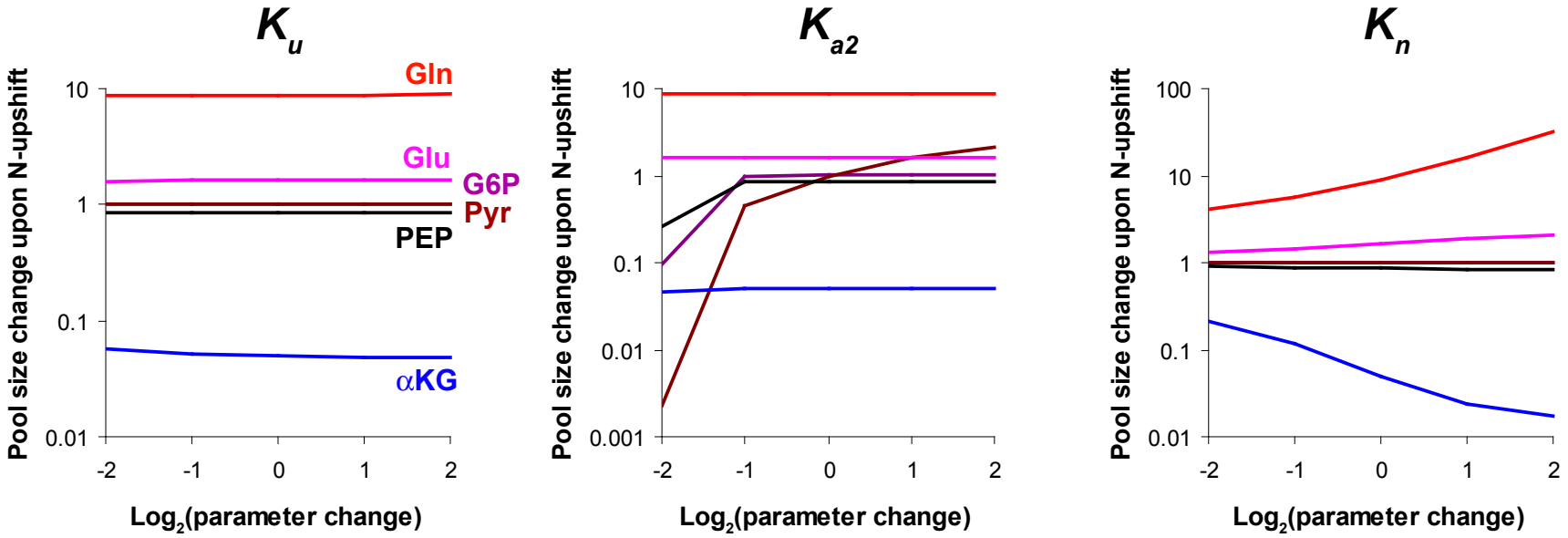

Supplementary Figure 5. Robust homeostasis of simulated glycolytic intermediate pools. The steady-state metabolite pool sizes were calculated as in Figure 4 of the main text after a multiplicative perturbation, ranging from 0.25 to 4, to one model parameter. Each panel depicts the fold-change in pool size upon a 13-fold increase in nitrogen availability (value at $S_N = 4.55$ divided by value at $S_N = 0.35$) as a function of the parameter perturbation. A horizontal line therefore indicates that a metabolite's response to nitrogen upshift is robust to changes in that parameter. The parameters selected here each represent the strength of one product feedback – K_u for glutamate, $K_{\alpha 2}$ for α-ketoglutarate, K_n for glutamine – and serve as examples of the three major parameter-sensitivity trends observed in the full parameter set: (1) no metabolites are sensitive; (2) G6P/Pyr/PEP are sensitive; (3) Gln/Glu/αKG are sensitive. See Supplementary Methods for descriptions of the parameters and more details on the parameter sensitivity analysis.

Supplementary Table 1. Growth rates of *E. coli* strains with arginine or aspartate as nitrogen source.

Strain	Growth rate, Arg (hr^{-1})	Growth rate, Asp (hr^{-1})
NCM 3722	0.341 ± 0.009	0.656 ± 0.032
NCM 3722 Δ*gltD*	N.D.*	0.274 ± 0.010
W3110	N.D.*	0.279 ± 0.007
VH33	N.D.*	0.215 ± 0.004

Cells were grown in media containing either 2.5 mM arginine or 10 mM aspartate as nitrogen source. Values are mean and standard error (n = 3). N.D.*: Not Determined due to insufficient growth following inoculation and growth overnight.

Supplementary Table 2. α-ketoglutarate concentration under various nitrogen conditions with mannitol as carbon source.

Nitrogen content of media	α-ketoglutarate concentration (mM)
10 mM NH_4Cl	0.497 ± 0.04
2 mM NH_4Cl	9.81 ± 0.62
Following upshift from 2 to 10 mM NH_4Cl	0.616 ± 0.04

Metabolites were extracted from mid-logarithmic phase *E. coli* filter cultures grown in media containing 4 g/L mannitol and the specified amount of NH_4Cl; extracts were analyzed by triple-quadrupole LC/MS-MS as described in Methods in the main text. The upshift from 2 mM to 10 mM NH_4Cl plates lasted 8 minutes before extraction, and was performed analogously to the experiment depicted in Figure 1 of the main text. The α-ketoglutarate peak areas from 4 replicates per condition were averaged and normalized by optical density of the culture, and the α-ketoglutarate concentration in each condition was then determined by the ratio of the normalized signal to that from cells growing in 4 g/L glucose and 10 mM NH4Cl, using the previously determined α-ketoglutarate concentration of 0.443 mM reported for that condition in Bennett et al. 2009[2].

Supplementary Methods

Metabolite extraction and measurement

Cells were grown in liquid batch culture to OD_{650} 0.1 and then transferred to nylon filters, which were placed on solid agarose media containing 2 mM NH_4Cl. The filter cultures were allowed to grow to OD_{650} 0.4, at which time the surface ammonia is depleted and cells are mildly nitrogen limited (as indicated by a reduced growth rate which recovers when the cultures are transferred to fresh agarose media[3]). At $t = 0$ the filters were transferred to solid media containing 10 mM NH_4Cl. At various times before and after the switch to ample ammonia, filters were rapidly submerged in cold organic solvent (-75 °C methanol or -20 °C 40:40:20 acetonitrile:methanol:water with 0.1% formic acid) to quench and extract metabolites. The extracts were analyzed by electrospray ionizationtandem mass spectrometry on a Thermo Quantum triple quadrupole mass spectrometer (Thermo Fisher Scientific, Inc.) operating in selected reaction monitoring mode, following liquid chromatography separation (LC-MS/MS), as described previously[4]. The values reported in Figure 1 are the fold changes in peak height compared to cells grown continuously on media containing 10 mM NH_4Cl. Absolute concentrations reported in Figures 2c and 3c were obtained by multiplying these fold changes by the absolute steady-state concentrations determined for this media formulation[2].

Model Definition

The equations governing our simplified model are shown below. The pool sizes of various intermediates are denoted as follows: G6P = x_6; PEP = x_p; Pyr = x_y; Glu = x_u; Gln = x_n; α-KG = x_α. The two input sources, glucose (carbon) and NH_3 (nitrogen), are denoted by S_C and S_N, respectively. There are two main types of factors controlling the flux into or out of each pool. The first is a Michaelis-Menten activation function, and the second is product-feedback inhibition. The differential equations describing the stoichiometry of the system are

$$
\begin{aligned}
\frac{dx_6}{dt} &= I_1 - V_1 \\
\frac{dx_y}{dt} &= I_1 - V_2 \\
\frac{dx_p}{dt} &= 2V_1 - I_1 - V_2 \\
\frac{dx_\alpha}{dt} &= V_2 - V_3 \\
\frac{dx_u}{dt} &= 2V_3 - I_2 - G \\
\frac{dx_n}{dt} &= I_2 - V_3
\end{aligned}
$$

and the various fluxes on the right hand sides are defined as

$$
\begin{aligned}
I_1 &= S_C \frac{K_\alpha}{x_\alpha + K_\alpha} \frac{x_p}{K_{imp} + x_p} \\
V_1 &= U_{6p} \frac{x_6/K_6^m - (x_p/K_p^m)^2}{1 + (x_p/K_p^m)^2 + x_6/K_6^m} \\
V_2 &= U_{yp} \frac{K_{\alpha 2}}{x_\alpha + K_{\alpha 2}} \frac{x_y}{K_y^m + x_y} \frac{x_p}{K_{p2}^m + x_p} \\
V_3 &= U_{an} \frac{K_u}{x_u + K_u} \frac{x_\alpha}{K_\alpha^m + x_\alpha} \frac{x_n}{K_n^m + x_n} \\
G &= \frac{G_0}{\frac{K_n^g}{x_n} + \frac{K_\alpha^g}{x_\alpha} + 1} \\
I_2 &= S_N \frac{K_n^2}{x_n^2 + K_n^2} \frac{x_u}{K_u^m + x_u}
\end{aligned}
$$

In our simplified model, the terms I_1 and I_2 represent carbon and nitrogen input fluxes, respectively. Note that, importantly, α-KG provides feedback inhibition to I_1 (reflecting α-KG inhibition of citrate synthase[5]) and Gln provides feedback inhibition to I_2 (reflecting Gln feedback inhibition of glutamine synthetase[6]). The term V_1 was chosen to give the proper ratio of G6P and PEP pool sizes in the absence of other inputs. The term V_2 corresponds to production of α-KG from PEP and Pyr, while V_3 corresponds to production of Glu from α-KG and Gln. Also note that we have chosen the growth term, G, to be regulated by *both* α-KG and Gln while the actual growth substrate is exclusively Glu. Although there exist many detailed models of glycolysis and the PTS[7,8], the utility of this simplified model is in demonstrating, with as few complicating details as possible, that our proposed feedback

mechanism can indeed provide the hypothesized link between carbon and nitrogen import with minimal change in the steady-state pool sizes of carbon intermediates.

The parameter values used were: $S_C = 1.1; K_\alpha = 50; K_{\alpha 2} = 50; K_p^m = 0.1; K_{p2}^m = 0.1; K_{imp} = 0.1; U_{6p} = 3; K_6^m = 0.1; U_{yp} = 3; K_y^m = 0.1; U_{an} = 3; K_u = 1; K_a^m = 0.05; K_n^m = 2.5; K_n = 3; K_u^m = 0.05; K_\alpha^g = 0.2; K_n^g = 1.5; G_0 = 1$. Nitrogen availability, S_N, was chosen to be .35 pre-upshift and 4.55 post-upshift. Because we consider only steady-state relative pool sizes pre- and post-upshift, the parameters are all given in dimensionless units and we do not imply a direct relationship between model parameters and their nearest in vivo equivalent.

The dynamics above contain a *sum rule*, specifically a linear combination of carbon intermediates which remains constant in time: 2[G6P] + [PEP] − [Pyr] = a constant. If we begin with initial conditions such that the constant > 0, this will remain true at all times. If the cell experiences carbon limitation, the intracellular pool sizes will shrink until Pyr is near zero, but there will always remain a pool of PEP due to the sum rule. We only need to take care to start the system with the constant > 0.

Sensitivity Analysis

By varying the values of individual parameters we determined which qualitative and quantitative features of the model are sensitive to which parameters (see Supplementary Fig. 3). There are three broad classes of parameters: those whose values have little or no effect on any quantity in the model (K_y^m, K_a^m, K_u^m, K_u); those whose values affect homeostasis of glycolytic intermediates (K_α, $K_{\alpha 2}$, K_p^m, K_{p2}^m); and those whose values affect the quantitative response of nitrogen assimilation intermediates (all others). Specific values for this last group were chosen so that the fold-change in growth rate and pool sizes upon a 13-fold change in external nitrogen matches experimental obervations.

Two of the parameters that affect glycolytic homeostasis control the strengths of α-KG feedback inhibition on glucose import (K_α) and on its own production ($K_{\alpha 2}$). α-KG must control most of the regulation of the carbon reactions to maintain nearly constant pool sizes of glycolytic intermediates. This requires the feedback inhibition constants K_α and $K_{\alpha 2}$ to be roughly equal, so that the regulation of I_1 and V_2 occur in parallel without requiring changes in other pools. The known K_i of α-KG with respect to citrate synthase (0.7 mM)

is not far from the K_i we determined for Enzyme I (1.3 mM), so the assumption that the corresponding parameters in our simplified model are equal in value is reasonable[5]. The other two parameters affecting glycolytic homeostasis, K_p^m and K_{p2}^m, control the extent of PEP saturation of the two reactions consuming that metabolite (glucose transport and α-KG production).

Supplementary References

1. Teplyakov A. *et al*. Structure of phosphorylated enzyme I, the phosphoenolpyruvate:sugar phosphotransferase system sugar translocation signal protein. *Proc. Natl. Acad. Sci. U. S. A.* **103**(44):16218-16223 (2006).
2. Bennett B.D. *et al*. Absolute metabolite concentrations and implied enzyme active site occupancy in Escherichia coli. *Nat Chem Biol*. **5**(8):593-599 (2009).
3. Yuan J. *et al.* Metabolomics-driven quantitative analysis of ammonia assimilation in E. coli. *Mol. Syst. Biol.* **5**, 302 (2009).
4. Lu W., Bennett B.D. & Rabinowitz J.D. Analytical strategies for LC-MS-based targeted metabolomics. *J. Chromatogr., B; Anal. Technol. Biomed. Life Sci.* **871**, 236-242 (2008).
5. Pereira D.S., Donald L.J., Hosfield D.J. & Duckworth H.W. Active site mutants of Escherichia coli citrate synthase. Effects of mutations on catalytic and allosteric properties. *J Biol Chem*. **269**(1):412-417 (1994).
6. Jiang P., Mayo A.E. & Ninfa A.J. Escherichia coli Glutamine Synthetase Adenylyltransferase (Atase, EC 2.7.7.49): Kinetic Characterization of Regulation by PII, PII-UMP, Glutamine, and α-Ketoglutarate. *Biochemistry* **46**(13):4133-4146 (2007).
7. Chassagnole C., Noisommit-Rizzi N., Schmid J.W., Mauch K. & Reuss M. Dynamic modeling of the central carbon metabolism of Escherichia coli. *Biotechnol Bioeng*. **79**(1):53-73 (2002).
8. Rohwer J.M., Meadow N.D., Roseman S., Westerhoff H.V. & Postma P.W. Understanding glucose transport by the bacterial phosphoenolpyruvate:glycose phosphotransferase system on the basis of kinetic measurements in vitro. *J Biol Chem*. **275**(45):34909-34921 (2000).